Emergent Materials
https://doi.org/10.1007/s42247-023-00533-9

ORIGINAL ARTICLE

Electrospun composite nanofibers for treating infectious esophagitis

Muge Koyun[1,2] · Rabia Betul Sulutas[1,2] · Yigit Turan[1,2] · Hatice Karabulut[1,2] · Armaghan Moradi[1,3] · Huseyin Berkay Ozarici[1] · Songul Ulag[1,4] · Ali Sahin[5] · Mehmet Mucait Guncu[6] · Oguzhan Gunduz[1,4]

Received: 29 March 2023 / Accepted: 28 June 2023

Abstract
The electrospinning technique enables the convenient fabrication of non-woven fibrous materials with excellent properties such as fine diameters, a large surface area per unit mass, high porosity, high gas permeability, and small pore sizes. Nanofiber applications in healthcare systems continue to be popular especially in recent years and are integrated with drug delivery systems in the treatment of diseases such as infectious esophagitis. For that reason, in this study, 13% polyvinyl alcohol (PVA), 0.5% gelatin (GEL), and 5, 10, and 15 mg of fluconazole (FCZ) were used to fabricate the drug-loaded nanofibers using the electrospinning method for local treatment of infectious esophagitis. The SEM images demonstrated the fibers' homogeneous and beadless morphologies and the mean diameter of electrospun nanofibers ranged between 395±12 nm and 314±93 nm. With the addition of FCZ, the properties of electrospun nanofibers improved, and some shifts in FTIR peaks were observed. The thermal properties of the electrospun nanofiber were also improved, and the highest melting temperature of PVA was observed at 235 °C when the drug concentration was highest. The tensile strength of 13% PVA/0.5% GEL/15 FCZ electrospun nanofibers was the highest and resulted in 7.07±1.33 MPa. Moreover, the biocompatibility of electrospun nanofibers was tested on MSC cells, which were able to spread all over the electrospun nanofibers even on day 7, due to the biocompatibility of each electrospun nanofibers. In addition, the antimicrobial and drug release kinetics properties of the FCZ-loaded electrospun nanofiber patches were tested against *S. aureus*, *S. agalactia*, and *C. albicans.*

Keywords Electrospinning · Esophagitis · Fluconazole · Infectious esophagitis · Nanofiber · Tissue engineering

1 Introduction

Esophageal cancer is the sixth leading cause of cancer death, affecting over 450,000 people worldwide [1]. The removal of cancer-affected tissue and replacement with autologous tissue from the patient's colon or stomach is one of the treatments used; however, undergoing this invasive surgery may result in medical complications such as increased infection risk, stenosis, and anastomotic leakage [2]. Infectious esophagitis (IE) is an infection-induced inflammation of the esophagus usually seen in patients with a weakened immune system due to either diseases or treatments such as cancer, chemotherapy, or surgery. It is critical to treat this condition properly since it is frequently observed in response to comorbidities or immunosuppressive medications [3].

Having mentioned the concerns in cancer therapy, the necessity for tissue engineering technologies is now greater than ever to replace excised tissue with innovative synthetic materials that can enable repair or duplication of the function of the esophagus while lowering the possibility of subsequent complications linked to infections. A successful esophageal reconstruction requires an ideal material replacement that provides a suitable environment for muscle regeneration and mucosal formation. Additionally, the substitute material must match the esophagus anatomically, physiologically, and functionally. Moreover, it must have high elasticity and strength, comparable to the natural esophagus [4], and be capable of enduring pressures induced by food and peristalsis; subsequently, the utilized material after transplantation should not cause infection, inflammation, stenosis, or fluid leakage [5]. The most crucial property of scaffolds in tissue engineering is their interconnected porous

Highlights
1. The use of the three materials for the treatment of infectious esophagitis has not yet been reported using the electrospinning method.
2. Nanofibrous scaffolds were successfully manufactured and demonstrated biocompatibility with mesenchymal stem cells.
3. The fluconazole addition increased the mechanical properties of the nanofibers.

Extended author information available on the last page of the article

Published online: 17 July 2023

structure with a high surface area that supports cellular adhesion, proliferation, and migration during tissue development. Besides, during tissue remodelling, the scaffolds should be biodegradable and resorbable [2]. The chosen material plays a vital role in the success of engineered tissue; thus, the most promising materials for tissue engineering are biodegradable polymers with high degradation, drug delivery ability, and mechanical strength properties [6].

Along with biodegradable polymers, the electrospinning method enables the simple and scalable manufacturing of porous nanofibers with superior tensile strength compared to other nanofiber fabrication techniques such as molecular self-assembly and temperature-induced phase separation. Electrospinning is the process of removing a viscous polymer solution from the liquid surface in an electric field created by high-voltage power. During this process, the liquid is delivered to the tip of the conductive needle at a constant flow rate. When the surface tension of the liquid is below the electrostatic force, the solution drops at the needle tip, forming the "Taylor cone" as a result of deformation. A jet occurs at the point where the voltage applied from the power source exceeds the critical value of the surface tension of the liquid. During this time, volatile solvents in the polymer solution evaporate, and long and thin fiber filaments are ejected from the jet. Microstructured and nanostructured fibers formed in the electric field accumulate around the collector and form a homogeneous fiber surface [7]. There are many different factors that affect the electrospin process. Parameters such as the molecular weight of the polymer, the chemical properties of the polymer solution, the applied electrical field density, the distance between the needle that transmits the solution and the collector, the humidity in the environment, temperature conditions, an open system, and a closed system have properties that can directly affect the result of the study, either positively or negatively. Fiber diameter, porosity, morphology, mechanical strength, biocompatibility, surface adhesion, and pore size vary and develop depending on these parameters [8]. The simplicity of producing submicron-sized fiber scaffolds with high tensile strength is a significant advantage of electrospinning over other widely utilized tissue engineering methods such as 3D printing [9]. Various scaffolds for esophageal reconstruction have been produced, as well as several resorbable materials, acellular matrices, and natural and synthetic polymers, each with advantages and limitations [3]. The esophagus consists of mucosal, submucosal, muscular, and adventitial layers, making it a complex multi-layered structure to mimic; hence, the need for the development and production of novel materials for each layer should be carefully considered [10].

Park et al. investigated a study in 2020 to explore the potential of electrospun polyurethane nanofibers and 3D-printed PCL scaffolds for esophageal tissue engineering applications by implanting them into a partial esophageal defect rat model; the purpose of this study was to assess the potential of human adipose-derived mesenchymal stem cells (ADSC) in tissue regeneration, by characterizing scaffolds with and without seeded ADSCs [3]. They claimed no indication of a substantial change because of ADSC seeding. Furthermore, they observed that PU nanofibers are more effective for re-epithelialization than 3D-printed scaffolds for muscle regeneration. In previous work, Barron et al. (2018) explored using polyurethane-based electrospun nanofibers seeded with mucosal cells for full-thickness regeneration of a 5-cm-long gap in a pig model [11]. Both seeded and unseeded PU scaffolds could initiate full-thickness regeneration of the esophagus. They observed that full-thickness regeneration in the pig model indicated a promising therapeutic use of PU electrospun nanofibers for humans. In 2022, Qin et al. examined the improvement of nylon/silk fibroin nanofiber mats by depositing chitosan and collagen via layer-by-layer self-assembly [12]. They observed that the modified material outperformed the mechanical strength of the esophagus, enhanced its biocompatibility, and inhibited gram-positive and gram-negative bacterial growth for more than 90%.

Despite past studies demonstrating the feasibility of tissue engineering using electrospun nanofibers of synthetic polymers to replace esophageal tissue in non-immunocompromised animals, little work has been done on decreasing the side effects, such as infection and inflammation [13]. We hypothesize that an anti-infective drug additive could benefit the nanofiber scaffold with a mixture of highly stable polymers PVA and gelatine to reduce the infection risks associated with esophageal reconstruction using synthetic materials. Gelatine, a collagen derivative, can mimic the musculo-cartilaginous structure of the esophagus due to its excellent biocompatibility, bioactivity, and biodegradability. Polyvinyl alcohol (PVA) provides structural stability and mechanical strength because of its superior hydrophilic and biocompatible properties [14]. Meanwhile, gelatine's well-known drug delivery functionalities and resemblance to the extracellular matrix can help with biocompatibility enhancement [15]. We fabricated and studied unique electrospun fluconazole-loaded PVA/gelatine nanofibers for potential application as a synthetic tissue-engineering scaffold to restore the structure and function of diseased esophageal tissue. After introducing an antifungal agent directly into nanofibers through the electrospinning solution, the material was further examined for its anti-infective efficacy, mechanical characteristics, and biocompatibility.

2 Materials and method

2.1 Materials

Polyvinyl alcohol (MW= 89,000–98,000 g/mol) and gelatin (from bovine skin, type B) were bought from Sigma-Aldrich (Saint Louis, MO, USA). Fluconazole (MW=306.27 g/mol) was obtained from Supelco®Analytical Products (Merck, KGaA, Germany). 3 wt% of Tween 80 (viscous liquid, CAS: 905-65-6) was purchased from Sigma-Aldrich, Taufkirchen, Germany. Phosphate buffer saline (PBS) (pH 7.4) was obtained from Chembio (Istanbul, Turkey).

2.2 Preparation of the solutions

In this study, polyvinyl alcohol and gelatine were used as the main components of electrospun nanofibers. 2.6 g of PVA polymer was first dissolved in 20 mL of distilled water for 30 min at 100 °C. After 13% PVA (w/v) was completely dissolved on a magnetic stirrer and cooled down to room temperature, 0.05 g of gelatine was added and mixed for an extra 30 min at 60 °C to obtain homogenous solutions. Approximately 5–6 drops of tween 80 were added to blend solutions. Three different drug concentrations of fluconazole were also added and mixed in the blend solutions at amounts of 5 mg, 10 mg, and 15 mg.

2.3 Fabrication of nanofibers using electrospinning

Each solution was transferred into a 10-mL plastic sterile syringe and connected to a syringe pump (NE-300, New Era Pump Inc., Toledo, OH, USA) to supply solutions to the electrospinning electrical field. Laboratory-scale electrospinning (Inovenso, Istanbul, Turkey) was used to fabricate the electrospun nanofibers. The volume of the solution in the syringe was noted. Then, the 18-gauge needle was attached to one side of the tube, and the other side was attached to a syringe. The collector was covered by paper, allowing the electrospun nanofiber to detach from it easily. The flow rate was set to 1 mL/h, and the voltage was adjusted to 26.5 kV. After the setup, electrospinning was started and ran for 2 h.

2.4 Morphological characterization using SEM

Scanning Electron Microscope (SEM, Evo LS 10, ZEISS) was used to examine the electrospun nanofiber morphology and surface characteristics. The distribution of electrospun nanofiber diameters in the tissue scaffold was assessed by measuring 100 electrospun nanofiber diameters with Image software (Olympus AnalySIS, USA).

2.5 Fourier transform-infrared spectroscopy (FTIR) analysis

The chemical composition of the sample was determined by Fourier's transform infrared spectrophotometer (FTIR, JASCO FT/IR-4700, Japan) in the transmission mode with 4 cm^{-1} resolution (32 scans) between 400 and 4000 cm^{-1}.

2.6 Differential scanning calorimetry (DSC)

Thermal properties of the fabricated electrospun nanofibers were analyzed using a differential scanning calorimetry (DSC, Shimadzu, Tokyo, Japan) device, with 25°C/min speed and at 25–400°C temperatures.

2.7 Tensile strength and deformation tests

Tensile strength tests were carried out for each sample using a Shimadzu (EZ-X, Tokyo, Japan) device at a speed of 5 mm/min and a force of 0.1N. Previously, the fabricated electrospun nanofibers were cut to 10-mm width and 50-mm length parameters. The samples' thicknesses were measured with a digital micrometer (Mitutoyo MTI Corp., USA) and recorded onto the program.

2.8 Swelling test

The swelling test was conducted periodically for seven days in phosphate-buffered saline (PBS) (pH 7.4) at 37°C, measuring the capacity of wound dressers' performance for water retention. Each sample was kept in 1 mL PBS solution at 37 °C in a thermal shaker incubator (BIOSAN TS-100). The weight of all scaffolds (W_0) was recorded for the first day. Wet sample weights (W_w) were recorded for 7 days. Furthermore, the swelling ratio (SR) of the fabricated electrospun nanofibers was calculated using the equation [16]:

$$\mathrm{SR} = \frac{W_T - W_0}{W_0} \times 100 \quad (1)$$

2.9 Drug release kinetic analyis

Each drug-loaded electrospun nanofiber was cut into small pieces, and 5 mg of each drug-loaded electrospun nanofiber was then submerged in 1 mL of phosphate buffer saline (PBS, pH: 7.4), and the samples were then incubated at 37 °C in a thermal shaker (BIOSAN TS-100) at 360 rpm. The FCZ drug release profile was measured at intervals of 15 min, 30 min,

60 min, and then at 1 h. PBS was measured using a UV-1280 spectrophotometer (SHIMADZU, 190–300 nm) following the time intervals. After each measurement, 1 mL of fresh PBS was added to the existing scaffolds for the following measurements. According to the previous study calibration curve and absorbance graph, cumulative drug release was plotted [17]. Different mathematical models, including zero-order (Eq. 2), first-order (Eq. 3), Korsmeyer-Peppas (Eq. 4), Higuchi (Eq. 5), and Hixson-Crowell (Eq. 6), were ere employed to estimate the FCZ drug kinetics release of the drug-loaded electrospun nanofibers, heir separate equations handed below [17]:

$$Q = K_0 t \tag{2}$$

$$\ln (1 - Q) = -K_1 t \tag{3}$$

$$Q = Kt^n \tag{4}$$

$$Q = K_h t^{1/2} \tag{5}$$

$$Q^{1/3} = K_{hc} t \tag{6}$$

In these equations, Q is the fractional amount of drug release at time t; K, K_0, K_1, K_h, and K_{hc} are the kinetic constants for each model. n indicates the diffusion exponent which indicate the drug release mechanism.

2.10 Antimicrobial test

S. aureus ATCC 29213, *S. agalactia* (beta-hemolytic streptococcus), and *C. albicans SC5314* were seeded on 5% sheep blood Columbia Agar (COS; Biomerieux, France) and McConkey Agar (MCK; Biomerieux, France) media with dilution seeding, respectively. They were stored in incubation overnight at 35 °C. On Mueller Hinton Broth medium (MHB; Biomerieux, France), 0.5 McFarland ($1–5\times10^8$ CFU/mL) bacterial turbidity suspensions were prepared and spread as a covering on the surface of Mueller Hinton E. Agar (MHE; Biomerieux, France). The discs were prepared by cutting each scaffold into a series of tiny (5 mm) circles. Which had been sterilized under UV light for 10 min before application and then placed on the solid medium at equal distances from each other. Additionally, all disc samples were placed on a sterile MHE agar medium for contamination evaluation. The formation of microorganisms around the circular discs was observed for contamination assessment.

2.11 MTT assay

Before being tested in cell culture, each electrospun nanofiber was sterilized using Class II Laminar flow for an overnight duration. The scaffolds were UV sterilized for an overnight period before being put into the 96-well plate with 20 µL DMEM. Incubation of the sterile electrospun nanofibers in DMEM growth media containing 10% FBS, 0.1 mg/mL penicillin/streptomycin, and 5% CO_2 took place for an hour at 37 °C. The electrospun nanofibers were collected, and the residual media were extracted with a micropipette. Human adipose-derived mesenchymal stem cells (hAD MSCs) and monolayer cells (2D) were seeded at a density of 1×10^3 cells per electrospun nanofibersduring the cell culture method, which was completed in a humid incubator at 37 °C with 5% CO_2. Using the MTT (3-[4,5-dimethylthiazol-2yl]-2,5-diphenyl-tetrazoliumbromide) 1116BEDIRET AL. cytotoxicity detection kit from Glentham Life Sciences, the cytotoxicity of the scaffolds was evaluated at a given time point. An Elisa reader was used to measure the cytotoxicity test's absorbance value at a wavelength of 560 nm (Perkin Elmer, Enspire). To get the precise figure, the test was conducted three times. The results were averaged to get the mean result. The growth media were removed from the plate after 1, 4, and 7 days of incubation, and cells on each electrospun nanofiberwere then fixed with 4% glutaraldehyde solution (Sigma-Aldrich) for SEM examination. Following that, ethanol was serially diluted and used to wash and dry each electrospun nanofibers at room temperature. After applying gold for 60 s at 10 kV to the dried scaffolds' surface, a SEM analysis of the morphology of the cell formations on the electrospun nanofibers was performed.

3 Results and discussions

3.1 Morphological characterization using SEM

The optimal concentration of polyvinyl alcohol (PVA) and gelatine (GEL) was determined based on previous research [18]. Therefore, in this study, the concentrations of PVA and GEL were kept the same. Only the fluconazole (FCZ) concentration was varied to observe the effect of the fluconazole in the treatment of infectious esophagitis. The morphological structure of the fabricated electrospun nanofibers can be seen in Fig. 1. As can be seen in Fig. 1a, homogenous and smooth electrospun nanofibers were obtained from the control group (13% PVA/0.5% GEL). Although there was no big difference in the mean diameter of the 13% PVA/0.5% GEL solution in the previous study, a smaller diameter of the 13% PVA/0.5% GEL solution was observed in our study. The mean diameter of the control group was observed at 352±85 nm whereas the mean diameter of the 13% PVA/0.5% GEL solution was measured at 395±12 nm in the previous study. However, with the addition of FCZ and even an increase in the amount of FCZ, a beaded structure was observed, which might be due to the viscosity change with the addition of fluconazole powder to the solution [19]. Beaded electrospun nanofibers formed as a result of

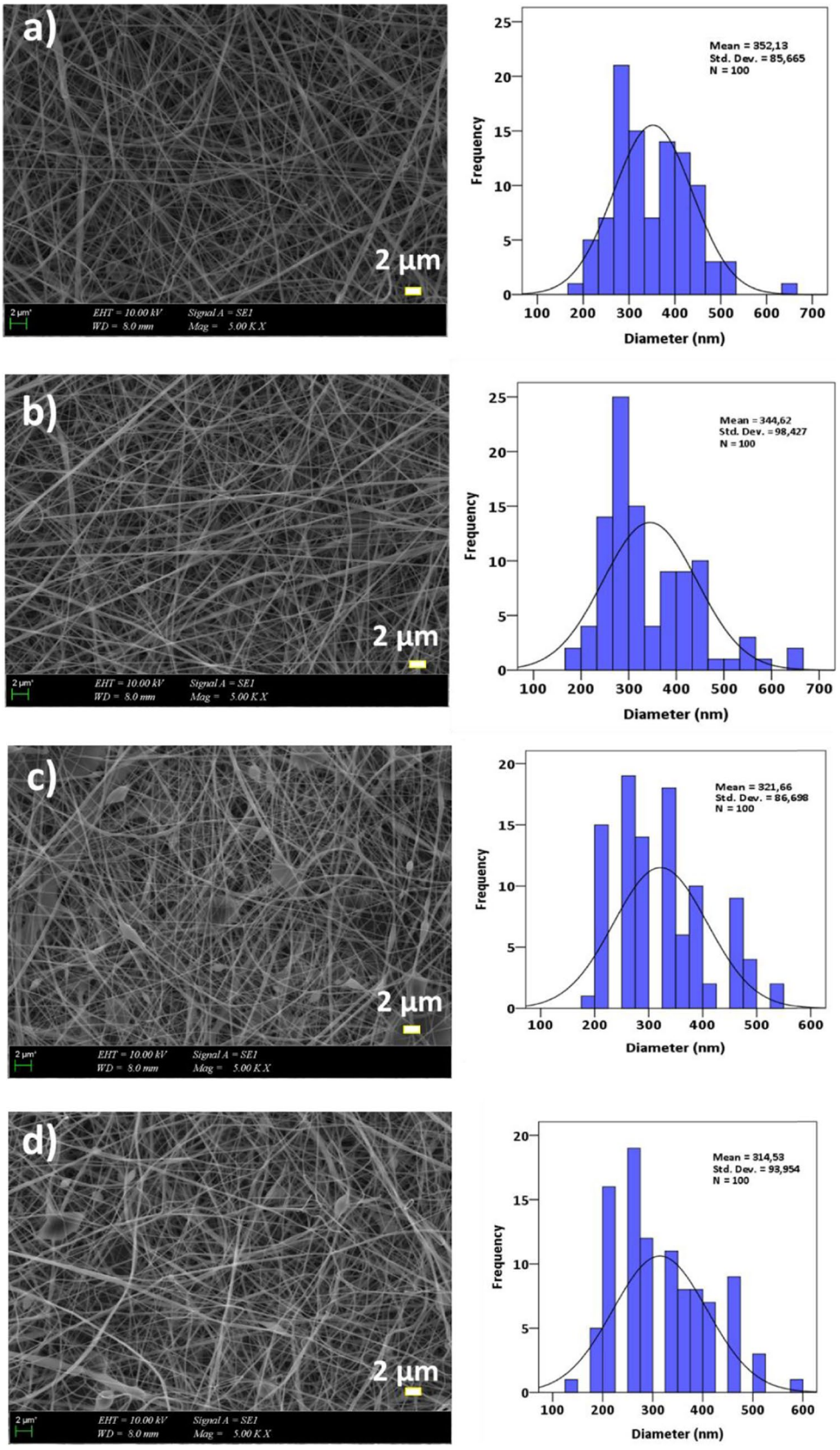

Fig. 1 SEM images of the nanofibers, 13% PVA/0.5% GEL (**a**), 13% PVA/0.5% GEL/5 FCZ (**b**), 13% PVA/0.5% GEL/10 FCZ (**c**), and 13% PVA/0.5% GEL/15 FCZ (**d**)

the viscosity change caused by the addition of FCZ, and the diameter of the electrospun nanofibers decreased. When the FCZ concentration was highest, the smallest mean diameter was observed at 314±93 nm, whereby the mean diameter of the electrospun nanofibers in 13% PVA/0.5% GEL/5 FCZ and 13% PVA/0.5% GEL/10 FCZ solutions was measured at 344±98 nm and 321±86 nm, respectively. To mimic the extracellular matrix of living tissue, it is crucial to create the same morphological structure of the extracellular matrix. Since polymeric electrospun nanofiber scaffolds can mimic and provide a suitable environment for cells, according to our SEM images in our study, we can say that our results showed that polymer electrospun nanofiber diameters at nanosize can successfully resemble the morphology of extracellular matrix [20].

3.2 Fourier transform-infrared spectroscopy (FTIR) analysis

FTIR analysis was performed to determine the functional groups and the components' interactions of the fabricated electrospun nanofibers. The FTIR spectra results of pure PVA-Gelatine consisting of 5, 10, and 15 mg of fluconazole electrospun nanofiber scaffolds are shown in Fig. 2. FTIR peaks of the control group (13% PVA/0.5% GEL) showed different peaks at 3288 cm^{-1}, 2908.13 cm^{-1}, 1421.28 cm^{-1}, 1326.79 cm^{-1}, 1141.65 cm^{-1}, 1089.58 cm^{-1}, 917.95 cm^{-1}, 840.81 cm^{-1}, and 516. 83 cm^{-1} indicating chemical bonds of PVA and gelatine polymers which might be resulted due to the stretching of hydroxyl groups, stretching of C—C, C—O, O—H, and C—H, bending of CH_2 vibrations as a result of PVA [20, 21]. It might also be related to the stretching of N—H band vibration, C=O stretching, and C—O stretching of secondary alcoholic groups and ester in gelatin [22]. With the addition of fluconazole, similar peaks were observed, and some shifts were observed at 3270.68 cm^{-1}, 1087.66 cm^{-1}, and 842.74 cm^{-1} because of new hydrogen bonds between intermolecular and intra-molecular bonds [23, 24]. In addition, new peaks were observed at 555.40 cm^{-1}, 503.33 cm^{-1}, and 485.97 cm^{-1} with the addition of FCZ. FTIR spectra results indicate that encapsulation of FCZ in the polymeric electrospun nanofibers was successfully achieved using the electrospinning method for the fabrication of electrospun nanofibers.

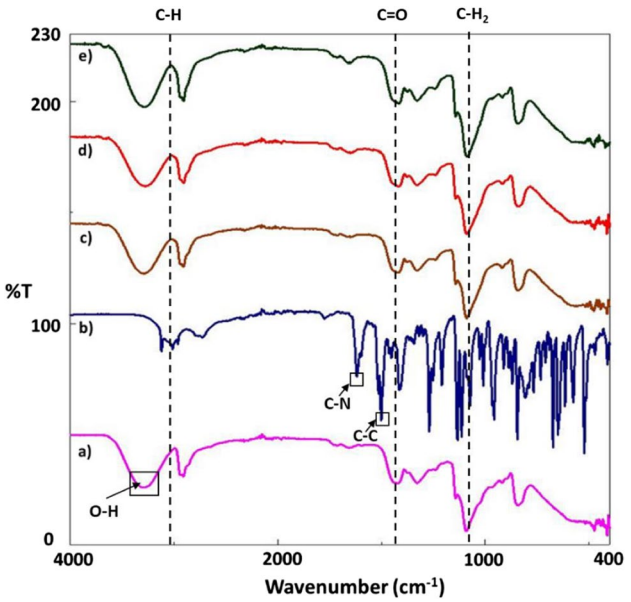

Fig. 2 FTIR peaks of the electrospun nanofibers, 13% PVA/0.5% GEL (**a**), pure fluconazole (FCZ) (**b**), 13% PVA/0.5% GEL/5 FCZ (**c**), 13% PVA/0.5% GEL/10 FCZ (**d**), and 13% PVA/0.5% GEL/15 FCZ (**e**)

3.3 Differential scanning calorimetry (DSC) analysis

DSC analysis was implemented to determine the thermal properties of the electrospun nanofibers and observe the crystallization and melting point of the polymers within the electrospun nanofibers. Thermal characteristics of each sample are shown in Fig. 3. A sharp peak was observed at 222 °C in the absence of FCZ. The peak at 222 °C can be resulted due to the melting point of PVA polymer within the electrospun nanofibers [25]. Thermal properties of the electrospun nanofibers improved with the increase in the amount of FCZ. Additionally, the melting point and glass transition temperature of PVA were observed in all samples. As shown in Fig. 3, even though there was no significant change in the the glass transition temperature of the PVA polymer, a slight increase in the glass transition temperature of PVA was observed around 55–60 °C [26]. However, the melting point of PVA polymer in the FCZ-loaded electrospun nanofibers was resulted in higher temperatures. After adding fluconazole with 5% and 10% concentration to PVA 13%, the melting

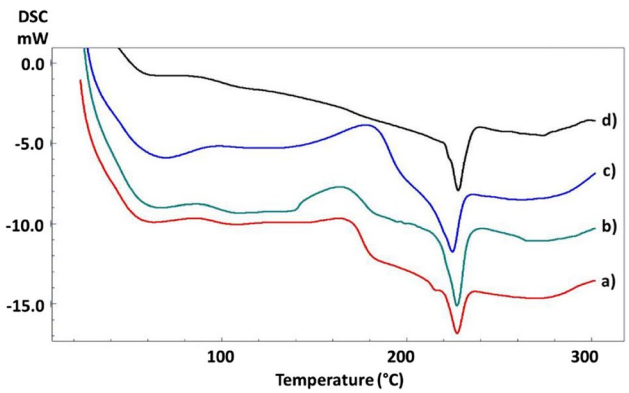

Fig. 3 DSC results of the nanofibers, 13% PVA/0.5% GEL (**a**), 13% PVA/0.5% GEL/5 FCZ (**b**), 13% PVA/0.5% GEL/10 FCZ (**c**), and 13% PVA/0.5% GEL/15 FCZ (**d**)

Table 1 Tensile strength and strain at break results of nanofibers

Nanofibers	Tensile strength (MPa)	Strain at break (%)
13% PVA/0.5% GEL	7.71±0.9	25.66±4.96
13% PVA/0.5% GEL/5 FCZ	6.95±0.28	20.30±3.10
13% PVA/0.5% GEL/10 FCZ	6.14±0.31	11.60±2.98
13% PVA/0.5% GEL/15 FCZ	7.07±1.33	36.04 ±4.97

point was increased to 225 °C and 227, respectively. The highest melting temperature of PVA was observed at 235 °C when the drug concentration was highest in the electrospun nanofiber. Thermal results of each sample show that each solution was perfeclty mixed and able to create the electrospun nanofibers from homegenous solutions.

3.4 Tensile testing results

The effect of FCZ drug addition on the mechanical properties of the nanofibers was investigated by tensile testing, and the tensile testing results for each electrospun nanofiber are given in Table 1. The control group had the highest tensile strength of 7.71±0.9 MPa but it can be seen that the tensile strength of the electrospun nanofibers was decreased compared to the control group with the addition of FCZ. The tensile strength of the 13% PVA/0.5% GEL/5 FCZ nanofibers was 6.95±0.28 MPa, whereas the tensile strength of the 13% PVA/0.5% GEL/10 FCZ electrospun nanofibers was 6.14±0.31 MPa. However, when the drug concentration was highest, surprisingly, the tensile strength of 13% PVA/0.5% GEL/15 FCZ electrospun nanofibers increased and resulted in 7.07±1.33 MPa. Tensile testing results, on the other hand, show that FCZ addition reduced the tensile strength of the electrospun nanofibers, which could be attributed to the beaded structure within the drug-loaded electrospun nanofibers [27, 28]. Even though the tensile strength of the 13% PVA/0.5% GEL/15 FCZ electrospun nanofibers was higher than that of other drug-loaded electrospun nanofibers, it is possible to assume that further studies might be needed to improve the mechanical properties of the electrospun nanofiber with the addition of FCZ with changing electrospinning parameters such as needle size, the distance between the capillary tip and the collector, applied voltage, and flow rate [29].

3.5 Swelling test results

The studies investigated in the literature showed that water absorption can be increased when the pore size and the porosity of the structure also increase. On the first 2 days of the swelling test, high water retention of the scaffold was observed (Fig. 4). Except for the material consisting of 13% PVA/0.5% GEL/10 FCZ, the swelling ratio was reduced in other scaffold samples in the following days. While the sample consisting of 13% PVA/0.5% GEL without fluconazole showed lower water retention capacity, compared to the other 3 samples with fluconazole, at the end of the 7th day, the scaffold consisting of 13% PVA/0.5% GEL/5 FCZ showed the highest water retention ratio. As a result of this observation, it can be concluded that drug and gelatin

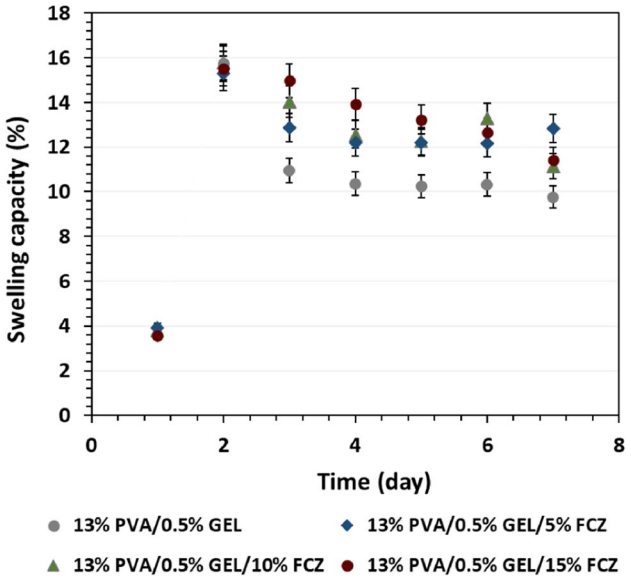

Fig. 4 Swelling rate of the nanofibers within several time intervals

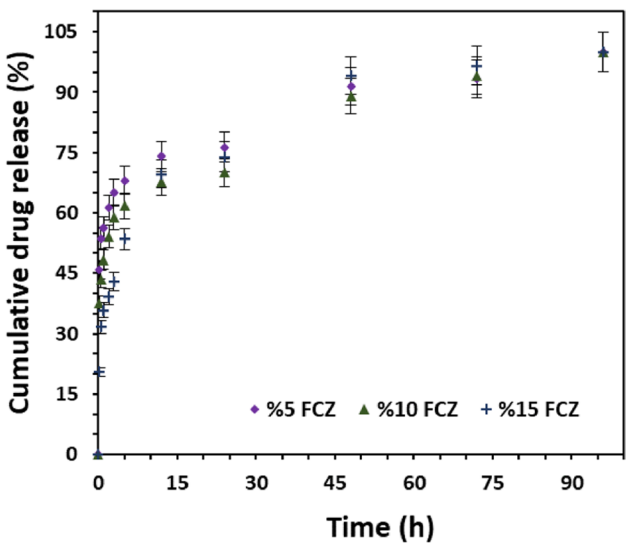

Fig. 5 Cumulative drug release kinetics of FCZ drug from drug-loaded nanofibers within several time intervals

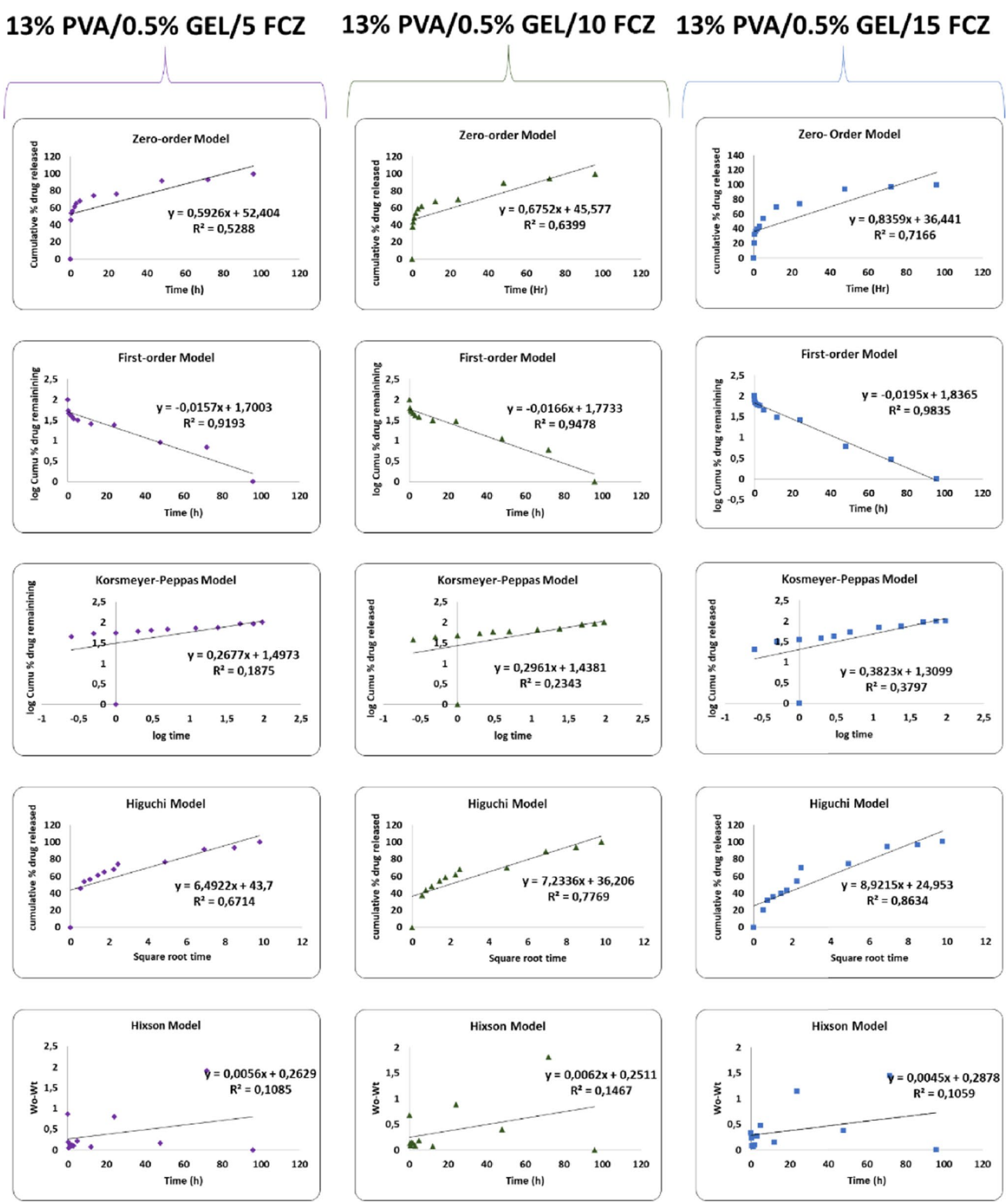

Fig. 6 Different drug release kinetic models of FCZ from drug-loaded nanofibers

loading can affect the capacity of water retention in scaffolds. As the swelling tests for pure PVA in the literature acknowledge, it is impossible to infer that PVA possesses a unique water retention characteristic. However, that can be advantageous for the application of polymeric electrospun nanofibers in tissue engineering and can enhance cell

Table 2 The inhibition zone diameters of the scaffolds and negative control groups

Samples	S. aureus ATCC 29213 (mm)	S. agalactiae (mm)	C. albicans SC5314 (mm)
13% PVA/0.5% GEL	0	0	0
13% PVA/0.5% GEL/5 FCZ	0	0	0
13% PVA/0.5% GEL/10 FCZ	0	0	0
13% PVA/0.5% GEL/15 FCZ	0	0	0
AM — ampicillin (2 µg)	19	-	-
NOR — norfloxacin	-	12	-
%20 chlorhexidine gluconate	-	-	26

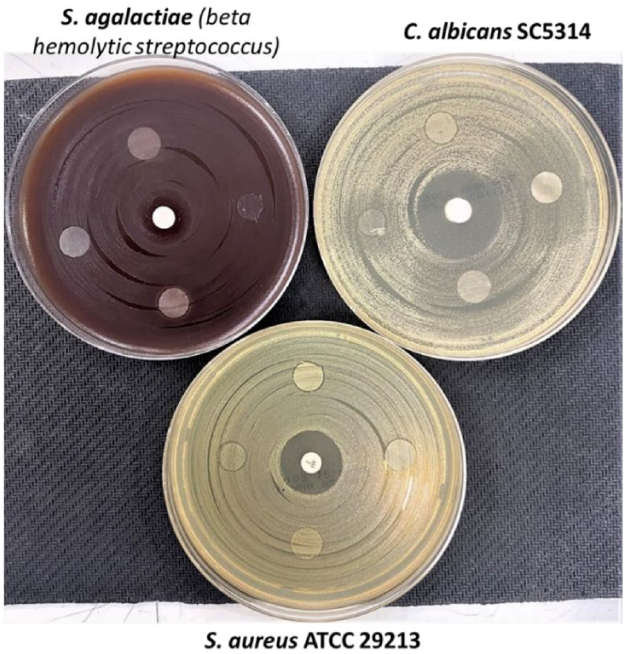

Fig. 7 The antimicrobial results of the electrospun nanofibers against *S. agalactiae*, *C. albicans* SC5314, and *S. aureus* ATCC 29213

adhesion [30]. Therefore, in order to promote cell adherence at an optimal rate, the use of hydrophilic PVA and gelatine polymers as components of electrospun nanofibers in this study was a highly favorable choice.

3.6 Drug release kinetics analysis

According to the drug release kinetics results, the 5% FCZ formulation has the highest cumulative amount among other concentrations, implying the maximum solubility in PBS. The time-dependent release profile of a drug has been observed and can be shown in Fig. 5. The drug in a sustained-release formulation can be delivered gradually and over a longer period, which is beneficial. Conversely, a fast-release formulation would show a more rapid release of the drug. By examining the cumulative amount released at different time points, the drug release format can be assessed. In this study, all three concentrations of fluconazole show a continuous increase in the cumulative amount released over time and lasted in 96 h. However, the release appears to be relatively faster for the 5% FCZ formulation compared to the 10% and 15% FCZ formulations. This suggests that the 5% FCZ formulation may lean more towards a fast-release profile, while the 10% and 15% FCZ formulations might exhibit a sustained-release pattern. Consequently, the saturated solubility of fluconazole in water appears to be the highest for the 5% FCZ formulation, and the drug release profiles indicate the possibility of a fast-release format for the 5% FCZ formulation and sustained-release formats for the 10% and 15% FCZ formulations. According to the study conducted by Nowak et al. (2019) investigated the effect of Soluplus® on fluconazole-loaded solid dispersions prepared using spray drying and fusion methods. The study found that the spray-dried sample exhibited slower drug release compared to crystalline fluconazole. This slower release was attributed to the slow diffusion of drug molecules from the thick polymer gel formed over the particles. Additionally, the solid dispersion with a drug carrier ratio of 10:90 remained stable in the amorphous state for 14 days [31]. These findings align with our results, where the drug release profiles showed a sustained release pattern over time. In another study focusing on the dissolution rate of fluconazole from solid dosage forms, the use of 3D printing techniques and the designed spatial structure of tablets led to fast tablet disintegration and dissolution. The tablets made from FLU40 filament exhibited the shortest disintegration times and released over 91% of the drug after 15 min. This finding suggests a fast drug release profile [32]. In our study, we observed a sustained release pattern, with the cumulative drug release increasing gradually over time. This difference in drug release profiles could be attributed to variations in the formulation, manufacturing technique, and excipients used in the solid dosage forms.

The concept of solid dispersions, initially proposed by Sekiguchi and Obi in the 1960s, involves the formation of solid products consisting of hydrophilic matrices and hydrophobic drugs. This approach is known to enhance drug absorption, solubility, and therapeutic effectiveness. Commonly used hydrophilic carriers include polyvinyl pyrrolidone (PVP), plasdone S-630, and polyethylene glycols (PEGs), while surfactants such as docusate sodium, Myrj-52, Tween 80, sodium lauryl sulfate, and Pluronic F-68 are sometimes incorporated during solid dispersion formation [33]. It is worth noting that the solubility enhancement techniques discussed in the literature align

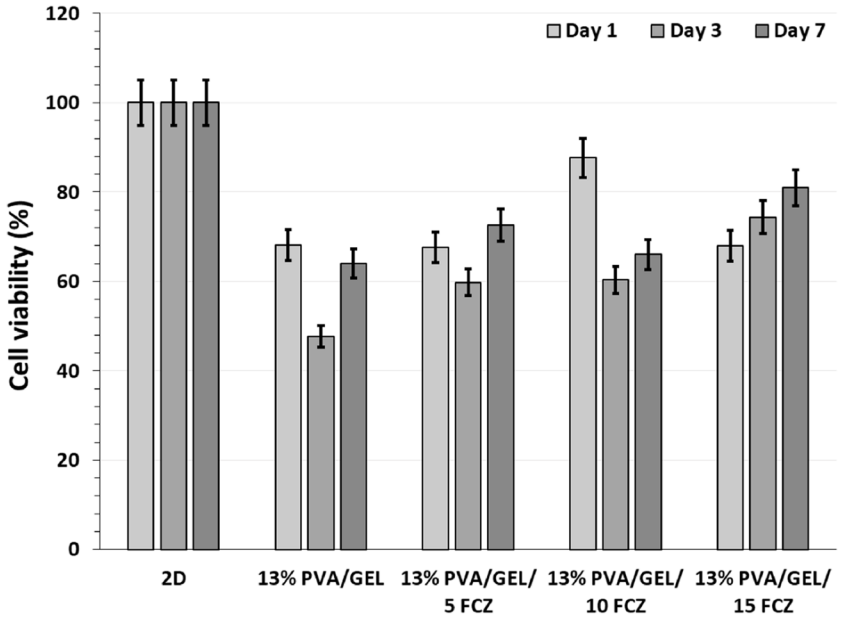

Fig. 8 Cell viability of the MSC culture on the fabricated electrospun nanofibers over different time intervals

with our research goal of improving the solubility and release profiles of fluconazole. Overall, research into the solubility and release characteristics of fluconazole and its solid dispersions has shown findings that match with ours. Variations in drug release patterns have been noted among studies; however, this may be due to changes in experimental settings, formulations, and methodologies.

Additionally, the release kinetics of FCZ drugs from drug loaded electrospun nanofibers were separately investigated with zero-order, first-order, Korsmeyer-Peppas, Higuchi, and Hixon-Crowell models, which are shown in Fig. 6. The most suitable mathematical model for the release kinetics of FCZ drugs was evaluated based on the highest correlation coefficient (R^2) value. According to the drug release kinetics of all drug-loaded electrospun nanofibers, the first-order kinetics model resulted in more appropriate behavior, which can help optimize the drug release kinetics of FCZ from electrospun nanofibers.

3.7 Antimicrobial test

Since fluconazole is an effective drug that can be used in the treatment of esophageal [34], it is important to test the antimicrobial test to observe the effect of FCZ-loaded electrospun nanofibers against *S. agalactiae*, *C. albicans* SC5314, and *S. aureus* ATCC 29213. Table 2 and Fig. 7 exhibit the antimicrobial activity of drug-loaded electrospun nanofibers against *S. agalactiae*, *C. albicans* SC5314, and *S. aureus* ATCC 29213. However, the concentration of the FCZ was not able to show an effect against these microorganisms which might be due to the quantities of FCZ or its extensive use, which may result in bacterial and fungal strains developing resistance to this medication [35]. Therefore, considering the antimicrobial results, it is possible to suggest that it will be reasonable to continue looking at changes in drug concentration.

3.8 Biocompatibility properties of the nanofibers

The use of drug-loaded electrospun nanofibers should focus on their applicability in biomedical applications. Therefore, we must first confirm that components of the scaffold do not pose a toxic effect on cells. Secondly, we need to show that the fabricated electrospun nanofibers promote cell proliferation and adhesion. For this purpose, the MTT assay was performed to observe cell viability on the scaffolds. Additionally, the cell viability of the electrospun nanofibers was tested using the MTT assay over different incubation times, and the results are shown in Fig. 8. Although there was no significant difference between the electrospun nanofibers even over different time periods, the highest cell viability was observed on the scaffold of 13% PVA/0.5% GEL/10 FCZ on day 1, which was approximately 88%, whereas the lowest viability of nearly 68% was observed on the scaffold when the drug concentration was lowest. On day 3, cell viability decreased slightly due to a lack of fresh nutrition. However, the viability of MSC cells on day 7 increased, and the highest cell viability was observed on the scaffold of 13% PVA/0.5% GEL/15 FCZ with 81% viability. Overall, the cell viability results confirmed that each electrospun nanofiber scaffold is biocompatible enough to keep cells alive and even proliferate over time. Moreover, electrospun nanofiber scaffolds have been proven to enable greater cell adhesion than film samples in previous studies. The MTT results in our study also indicate that the material choice of the scaffold and fabrication method of electrospun nanofibers were

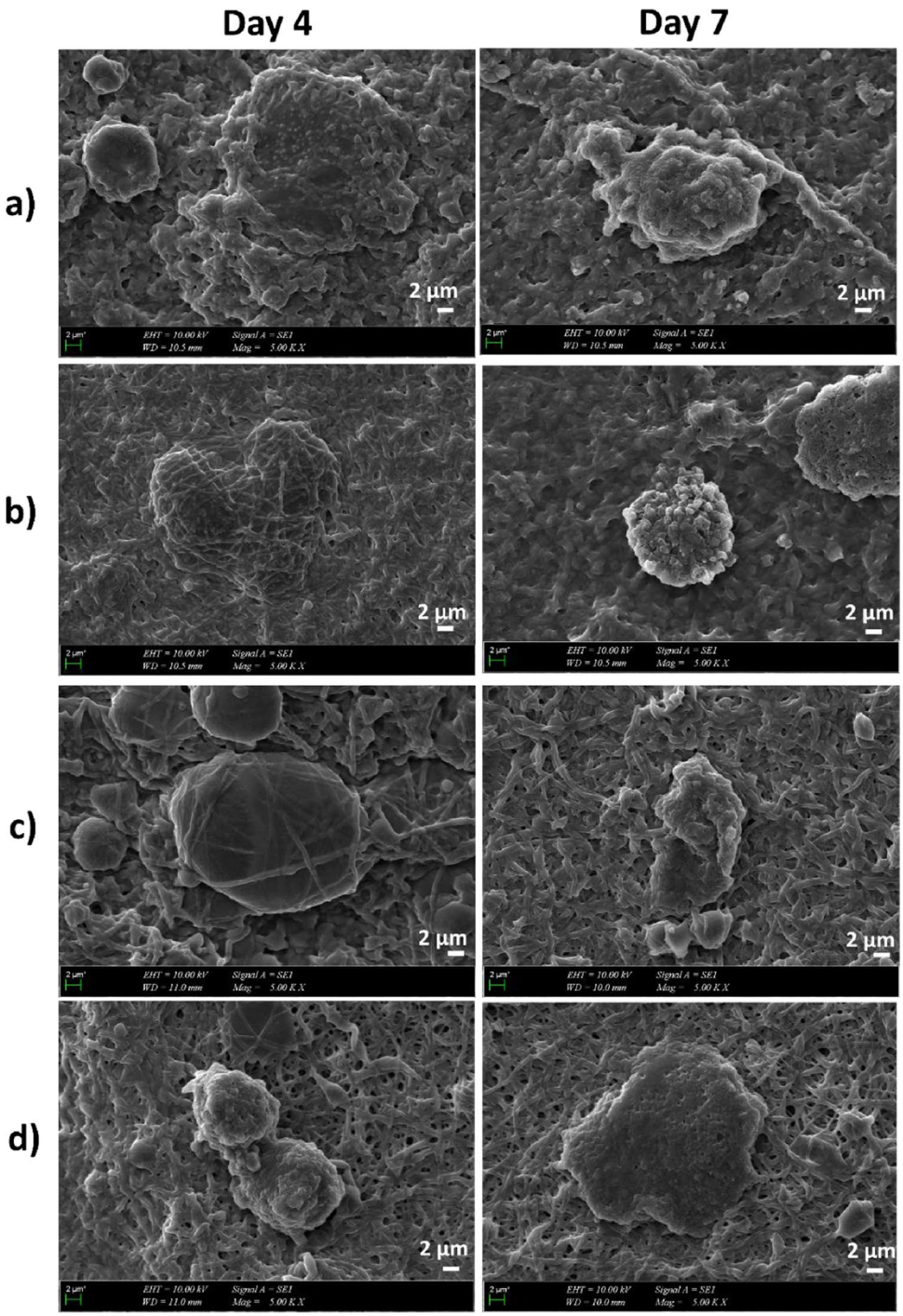

Fig. 9 MSC culture on the fabricated electrospun nanofibers over different time intervals

successful in providing an optimal environment for cells, which resulted in great cell viability on the scaffolds [36].

Figure 9 demonstrates the cell morphology on the electrospun nanofiber scaffolds at different period. As can be seen, cells were able to attach to the electrospun nanofiber scaffold and proliferate over time. When the results were compared with the drug concentration in the nanofiber scaffold, a slight change in the morphology of the MSC cells was observed. On day 4, the bigger cell structures were observed on the scaffold of 13% PVA/0.5% GEL and 13% PVA/0.5% GEL/10 FCZ. Furthermore, cells could spread all over the scaffolds even day 7. Similar cell structures were observed due to biocompatibility of each electrospun nanofiber scaffold. This demonstrated the importance of the electrospun nanofiber structure in promoting strong cell attachment simply because the nanoscale structure may provide cells with a three-dimensional environment [37].

4 Conclusions

In this study, the electrospinning technique was used to fabricate electrospun nanofiber scaffolds from PVA, gelatin, and FCZ drug for the treatment of infectious esophagitis since the remediation of infectious esophagitis requires a well-designed technique due to its local and severe disorder. The desired morphological structure of electrospun nanofibers was successfully fabricated with a varying diameter range of 395±12 nm and 314±93 nm and was able to mimic morphological structure of extracellular matrix at nanoscale. The FCZ drug was encapsulated in the electrospun nanofibers without forming beaded structures and slowly and controllably released within 96 h, which is crucial to preventing antibiotic resistance and the growth of microorganisms in the infected area. MSC cells were treated on each electrospun nanofiber sample, and visible and big cell morphology was obtained. Cells could attach and even spread all over the surface of the electrospun nanofibers structure due to its suitable and mimicked environment of living tissue. According to each test performed in this study and due to the biocompatibility, desired mechanical strength, good swelling capacity, and thermal properties of electrospun nanofibers, we believe that the fabricated electrospun nanofibers in the study can provide the necessary environment for the treatment of infectious esophagitis. Although FCZ did not result in an antimicrobial effect against *S. agalactiae*, *C. albicans*, and *S. aureus*, this study provides promising results for the fabrication of tissue engineered structures with excellent and optimal parameters

Declarations

Conflict of interest The authors declare no competing interests.

References

1. A. Pennathur, M.K. Gibson, B.A. Jobe, J.D. Luketich, Oesophageal carcinoma. Lancet. **381**(9864), 400–412 (2013)
2. K.S. Chian, M.F. Leong, K. Kono, Regenerative medicine for oesophageal reconstruction after cancer treatment. Lancet Oncol. **16**(2), e84–e92 (2015)
3. C.M. Wilcox, Overview of infectious esophagitis. Gastroenterol. Hepatol. **9**(8), 517–519 (2013)
4. I.G. Kim, Y. Wu, S.A. Park, H. Cho, J.J. Choi, S.K. Kwon, et al., Tissue-engineered esophagus via bioreactor cultivation for circumferential esophageal reconstruction. Tissue Eng. A. **25**(21-22), 1478–1492 (2019)
5. H. Park, I.G. Kim, Y. Wu, H. Cho, J.W. Shin, S.A. Park, E.J. Chung, Experimental investigation of esophageal reconstruction with electrospun polyurethane nanofiber and 3D printing polycaprolactone scaffolds using a rat model. Head Neck. **43**(3), 833–848 (2021)
6. N.T.B. Linh, B.T. Lee, Electrospinning of polyvinyl alcohol/gelatin nanofiber composites and cross-linking for bone tissue engineering application. J. Biomater. Appl. **27**(3), 255–266 (2012)
7. H. Liu et al., Recent progress of electrospun herbal medicine nanofibers. Biomolecules. **13**(1), 184 (2023). https://doi.org/10.3390/biom13010184
8. S.G. Kumbar, R. James, S.P. Nukavarapu, C.T. Laurencin, Electrospun nanofiber scaffolds: engineering soft tissues. Biomed. Mater. **3**(3), 034002 (2008). https://doi.org/10.1088/1748-6041/3/3/034002
9. C. Xie, Q. Gao, P. Wang, L. Shao, H. Yuan, J. Fu, et al., Structure-induced cell growth by 3D printing of heterogeneous scaffolds with ultrafine fibers. Mater. Des. **181**, 108092 (2019)
10. W. Farhat, F. Chatelain, A. Marret, L. Faivre, L. Arakelian, P. Cattan, A. Fuchs, Trends in 3D bioprinting for esophageal tissue repair and reconstruction. Biomaterials. **267**, 120465 (2021)
11. M.R. Barron, E.W. Blanco, J.M. Aho, J. Chakroff, J. Johnson, S.D. Cassivi, et al., Full-thickness oesophageal regeneration in pig using a polyurethane mucosal cell seeded graft. J. Tissue Eng. Regen. Med. **12**(1), 175–185 (2018)
12. J. Qin, J. Zhao, Y. Wu, L. Li, D. Li, H. Deng, et al., Chitosan/collagen layer-by-layer deposition for improving the esophageal regeneration ability of nanofibrous mats. Carbohydr. Polym. **286**, 119269 (2022)
13. S. La Francesca, J.M. Aho, M.R. Barron, E.W. Blanco, S. Soliman, L. Kalenjian, et al., Long-term regeneration and remodeling of the pig esophagus after circumferential resection using a retrievable synthetic scaffold carrying autologous cells. Sci. Rep. **8**(1), 4123 (2018)
14. M. Song, H. Yu, J. Gu, S. Ye, Y. Zhou, Chemical cross-linked polyvinyl alcohol/cellulose nanocrystal composite films with high structural stability by spraying Fenton reagent as initiator. Int. J. Biol. Macromol. **113**, 171–178 (2018)
15. C. Kalkandelen, S. Ulag, B. Ozbek, G.O. Eroglu, D. Ozerkan, S.E. Kuruca, F.N. Oktar, M. Sengor, O. Gunduz, 3D printing of gelatine/alginate/β-tricalcium phosphate composite constructs for bone tissue engineering. ChemistrySelect. **4**(41), 12032–12036 (2019)
16. S. Khan, V. Trivedi, J. Boateng, Functional physico-chemical, ex vivo permeation and cell viability characterization of omeprazole loaded buccal films for paediatric drug delivery. Int. J. Pharm. **500**(1-2), 217–226 (2016)
17. S. Cesur, E. Ilhan, E. Pilavci, R.B. Sulutas, M. Gurboga, O. Bingol Ozakpinar, et al., A novel strategy as a potential rapid therapy modality in the treatment of corneal ulcers: fluconazole/vancomycin dual drug-loaded nanofibrous patches. Macromol. Mater. Eng. **308**, 2200697 (2023)
18. S. Ulag, E. Ilhan, R. Demirhan, A. Sahin, B.K. Yilmaz, B. Aksu, et al., Propolis-based nanofiber patches to repair corneal microbial keratitis. Mol. **26**(9), 2577 (2021)
19. B. Kim, H. Park, S.H. Lee, W.M. Sigmund, Poly (acrylic acid) nanofibers by electrospinning. Mater. Lett. **59**(7), 829–832 (2005)
20. X.J. Loh, P. Peh, S. Liao, C. Sng, J. Li, Controlled drug release from biodegradable thermoresponsive physical hydrogel nanofibers. J. Control. Release **143**(2), 175–182 (2010). https://doi.org/10.1016/j.jconrel.2009.12.030
21. S.M. Pawde, K. Deshmukh, Characterization of polyvinyl alcohol/gelatin blend hydrogel films for biomedical applications. J. Appl. Polym. Sci. **109**(5), 3431–3437 (2008)
22. E.J. Shin, Y.H. Lee, S.C. Choi, Study on the structure and processibility of the iodinated poly (vinyl alcohol). I. Thermal analyses of iodinated poly (vinyl alcohol) films. J. Appl. Polym. Sci. **91**(4), 2407–2415 (2004)
23. L. Dai, J. Li, E. Yamada, Effect of glycerin on structure transition of PVA/SF blends. J. Appl. Polym. Sci. **86**(9), 2342–2347 (2002)

24. M. Sun, Y. Wang, L. Yao, Y. Li, Y. Weng, D. Qiu, Fabrication and characterization of gelatin/polyvinyl alcohol composite scaffold. Polym. **14**(7), 1400 (2022)
25. S. Wang, J. Ren, W. Li, R. Sun, S. Liu, Properties of polyvinyl alcohol/xylan composite films with citric acid. Carbohydr. Polym. **103**, 94–99 (2014)
26. H. Karabulut, S. Ulag, B. Dalbayrak, E.D. Arisan, T. Taskin, M.M. Guncu, et al., A novel approach for the fabrication of 3D-printed dental membrane scaffolds including antimicrobial pomegranate extract. Pharm. **15**(3), 737 (2023)
27. L. Liu, S.E. Kentish, Pervaporation performance of crosslinked PVA membranes in the vicinity of the glass transition temperature. J. Membr. Sci. **553**, 63–69 (2018)
28. T. Li, X. Ding, L. Tian, S. Ramakrishna, Engineering BSA-dextran particles encapsulated bead-on-string nanofiber scaffold for tissue engineering applications. J. Mater. Sci. **52**, 10661–10672 (2017)
29. B. Tarus, N. Fadel, A. Al-Oufy, M. El-Messiry, Effect of polymer concentration on the morphology and mechanical characteristics of electrospun cellulose acetate and poly (vinyl chloride) nanofiber mats. Alex. Eng. J. **55**(3), 2975–2984 (2016)
30. F. Chellat, M. Tabrizian, S. Dumitriu, E. Chornet, P. Magny, C.H. Rivard, L.H. Yahia, In vitro and in vivo biocompatibility of chitosan-xanthan polyionic complex. J. Biomed. Mater. Res. **51**(1), 107–116 (2000)
31. O. Gunduz, S. Ulag, Gentamicin and fluconazole loaded electrospun polymethylmethacrylate (PMMA) fibers as a novel platform for the treatment of corneal keratitis. Int. J. Polym. Mater. Polym. Biomater. **72**, 1–13 (2022)
32. H. Shirinzadeh, S. Süzen, N. Altanlar, A.D. Westwell, Antimicrobial activities of new indole derivatives containing 1, 2, 4-triazole, 1, 3, 4-thiadiazole and carbothioamide. Turkish J. Pharm. Sci. **15**(3), 291 (2018)
33. M. Nowak, M. Gajda, P. Baranowski, P. Szymczyk, B. Karolewicz, K.P. Nartowski, Stabilisation and growth of metastable form II of fluconazole in amorphous solid dispersions. Pharm. **12**(1), 12 (2019). https://doi.org/10.3390/pharmaceutics12010012
34. J. Pyteraf, W. Jamróz, M. Kurek, U. Bąk, J. Loskot, D. Kramarczyk, M. Paluch, R. Jachowicz, Preparation and advanced characterization of highly drug-loaded, 3D printed orodispersible tablets containing fluconazole. Int. J. Pharm. **630**, 122444 (2023). https://doi.org/10.1016/j.ijpharm.2022.122444
35. M.S. Arun Kumar, M. Rajesh, L. Subramanian, Solubility enhancement techniques: a comprehensive review. World J Biol Pharm Health Sci. **13**(3), 141–149 (2023)
36. X.H. Chu, X.L. Shi, Z.Q. Feng, Z.Z. Gu, Y.T. Ding, Chitosan nanofiber scaffold enhances hepatocyte adhesion and function. Biotechnol. Lett. **31**, 347–352 (2009)
37. K.M. Woo, V.J. Chen, P.X. Ma, Nano-fibrous scaffolding architecture selectively enhances protein adsorption contributing to cell attachment. J. Biomed. Mater. Res. A. **67**(2), 531–537 (2003)

Authors and Affiliations

Muge Koyun[1,2] · Rabia Betul Sulutas[1,2] · Yigit Turan[1,2] · Hatice Karabulut[1,2] · Armaghan Moradi[1,3] · Huseyin Berkay Ozarici[1] · Songul Ulag[1,4] · Ali Sahin[5] · Mehmet Mucait Guncu[6] · Oguzhan Gunduz[1,4]

✉ Songul Ulag
songul.ulag@marmara.edu.tr

[1] Center for Nanotechnology & Biomaterials Application and Research (NBUAM), Marmara University, Istanbul, Turkey

[2] Institute of Pure and Applied Sciences, Department of Metallurgical and Materials Engineering, Marmara University, Istanbul, Turkey

[3] Department of Biomedical Engineering, Bahcesehir University, Istanbul, Turkey

[4] Department of Metallurgical and Materials Engineering, Faculty of Technology, Marmara University, Istanbul, Turkey

[5] Genetic and Metabolic Diseases Research and Investigation Center, Department of Biochemistry, Faculty of Medicine, Marmara University, Istanbul, Turkey

[6] Institute of Health Sciences, Department of Microbiology, Marmara University, Istanbul, Turkey